Noise contribution to timing with fraction discriminators

V.V.Sushkov
University of California Riverside, IGPP
CA, 92521, USA, tel: +1 (909)787-3957 fax: +1 (909)787-4509
E-mail: Vitali.Souchkov@ucr.edu

Abstract
The noise contribution to timing with pulse discriminators processing a fraction of the detector signal amplitude is discussed. The types of discrimination techniques under study do not produce theoretical walk for varying amplitude signals with equal shapes. They are suitable for implementation in the readout of time of flight (TOF) system and tracker. The utilization of the pulse discrimination methods in the nanosecond range with low-noise front-end may require tentative search of the processor parameters to achieve better time resolution. Simulation methods that provide rapid and consistent evaluation of front-end noise contribution to the time resolution are discussed.

Introduction
The interest to on-chip realization of a pulse discriminators that employ constant or double signal fraction in large readout system for a collider experiment requires elaboration of evaluation methods of front-end noise contribution to timing. The choice among one or another realization of constant fraction discriminator (CFD) [1] or double fraction discriminator (DFD) [2] has to be done. Another motivation behind the presented study is to provide a designer with a reliable estimation of time resolution before the designing of a signal processor circuit starts. In this study a semi-analytical approach in evaluation of electronic noise contribution to time resolution is developed. The timing variance may be simulated by implementation of a macro and a goal function within the waveform analyzer of SPICE simulator for any of the above discriminators. Universality of the approach to the timing variance evaluation is outlined. The proposed evaluation principle provides a possibility to bypass a bulky procedure of carrying out parametric analyses of numerous runs with circuits representing delay lines (or their substitutions), fraction and signal difference otherwise needed to analyze time resolution dependence on the signal processor parameters. The simulation results are compared to the measured data for one front-end.

Signal processor modeling
Figure 1a shows usual representation of a processor involving CFD used in timing measurements. The signal is represented by a current source I(t) connected in parallel to the detector capacitor. For the noise analysis the front-end is represented by a two-port with transfer function A(ω) and equivalent noise generators of series and parallel noises at the input. Whatever the noise generators are the electronic noise may be described by voltage fluctuations with spectral density S(f) at the input node of a processor part representing CFD (the input impedance of discriminator is usually 50 Ohm). Positive polarity for the branch of fraction and inversion for the branch of delayed signal are assumed in Figure 1. The final results are independent of simultaneous signal polarity inversion for the branches of delay and fraction in CFD representation (such representation may also be found in literature). The arming provides a low limit for the range of processed amplitudes triggering the "enable" input of the comparator used for zero crossing detection. The level for arming is normally well above three standard deviations of the signal amplitude fluctuations at the discriminator input. First in this study only "true constant fraction timing" [3] is considered to simplify the discussion. Therefore the amplitudes of the signals at the input of CFD are assumed to depend only on the detected signal charge Q_{in} ; the shapes of the signals are equal. Let us write an expression for the signal waveform at the input of CFD as:

$$V(t) = E\phi(t), \quad (1)$$

where ϕ(t) is the waveform of the response corresponding to some reference charge (or energy) detected, E is a factor of proportionality for the reference amplitude. For the processor schematically presented in Figure 1a the timing variance due to the

electronic noise contribution may be expressed as follows:

$$\sigma_t^2 = \frac{\sigma^2{}_N}{E^2 \,|(\alpha\phi(t) - \phi(t-\tau))'_t\,|^2_{t=t_Z}}\ , \quad (2)$$

where electronic noise variance is divided by the square of the signal slope at the input the zero crossing detector at the moment of zero crossing t_Z. The denominator in equation 2 takes into account the difference of the input signal of CFD delayed by τ and the fraction α of the non-delayed signal.

Electronic noise at the input of CFD may be associated with stochastic train of the impulses with the waveform ψ(t) randomly distributed in time domain. The spectral density S(f) of this noise may be represented by [4]:

$$S(f) = 2\lambda\,|F(\psi(t))|^2, \qquad (3)$$

where λ is a coefficient responsible for the intensity of the stochastic train, F designates Fourier transformation and the factor 2 appears as a result of transfer to the domain of positive frequency f. The transfer function of the noise impulse to the input of zero crossing detector is the same as for the signal, i.e. the noise waveform ϕ_N(t) at this node may be defined by the expression:

$$\phi_N(t) = \alpha\psi(t) - \psi(t-\tau), \qquad (4)$$

where τ is delay of CFD. Therefore noise spectral density at the input of zero crossing detector may be presented by the expression:

$$S_N(f) = 2\lambda\,|F(\psi(t))|^2\,|(\alpha - \exp(-j\omega\tau)|^2, \quad (5)$$

Noise variance at the input of zero crossing detector is the integral of the above spectral density over the full frequency band. The variance may be represented as follows:

$$\sigma^2{}_N = \int_0^\infty S(f)(\sin^2(2\pi f\tau) + (\cos(2\pi f\tau) - \alpha)^2)df \quad (6)$$

The last expression characterizes noise variance in timing with CFD. The correspondence of the expression 6 to the result obtained in time domain may be recognized from formula given in [5].

Application of the model

The model discussed was utilized in the simulations of noise contribution to timing measurements with an improved version of the spectrometry front-end [6], the essential details of that are shown in Figure 2. The detector is represented by a capacitor C_d of 1000pF to approximate large area Si photodiode used in real application. PSPICE circuit simulator is used in the simulations discussed below. In order to find noise variance $\sigma^2{}_N$ the spectral density S(f) at the input of CFD is to be determined. Having found noise spectral density S(f) in only one simulation run of noise analysis in PSPICE, the variance at the zero crossing detector node may be evaluated with waveform analyzer Probe for any parameters of fraction and delay according to expression 6. In the presented modeling, $\sigma^2{}_N$ is simulated by implementation of a macro in which the parameter of delay is scanned for each fraction parameter of interest. This approach allows us to obtain full information about noise at the input of zero crossing detector after only one simulation run by using command files with macros corresponding to expression 6.

For the noise simulations the models of the for the shaper operational amplifiers were constructed to fit the specifications of their noise figures, the other models are taken from the supplement library.

Figure 3 present plots of noise variance as a function of delay for three parameters of fraction. The noise variances are simulated for two gain factors of the filter-amplifier.

Different dependencies of the noise variances $\sigma^2{}_N$ on delay with a fixed parameters of fraction were stored in different files. These data were used in the second simulation run (in the equivalent voltage sources of pwl form [7]) in the time domain transient analysis for the simulations of time resolution. For the time domain simulations the macro corresponding to the denominator of expression 2 is derived for current stimulus representing the detector signal shape (δ-shape in our discussion). The amplitude of the stimulus corresponds to charge (or energy) detected. The slope at the instant of zero crossing is defined by a goal function implementation in Probe (see appendix). Simulated time resolution dependencies on CFD delay are presented in Figure 4. Each curve in Figure 4 corresponds to fixed parameter of fraction. Time resolution dependencies in this figure are normalized to 1 MeV energy deposition in Si detector. The shape of the front-end response obtained in the time domain simulations corresponds to one observed experimentally (with 25ns peaking time). The variations of time

resolution in the region of plateau are of the order of 20% of the mean value, the fraction of 0.3 being the optimal one for this region. For the short delays one may improve time resolution by using a higher fraction (for instance 0.5). The contribution of the filter-amplifier noise is not negligible. Therefore time resolution dependends on the gain of the filter-amplifier. The simulated dependencies of time resolution are compared to the measured data in Figure 5. The results presented correspond to 50 MeV energy deposition in current δ-shape signal. The contribution of the CFD circuit noise and an optimistic modeling of the front-end noise may be responsible for the observed difference between the simulated results and the measured values.

The model extension

The principles used to model signal processor that employs CFD may be extended to comprise DFD pick-off technique (Figure 1b). The timing variance in this case may be routinely derived through noise correlation analysis independently from whatever technique of the time stamp derivation in the back-end is used. If each pick-off of the signal amplitude fraction is taken instantly the resulting expression is as follows:

$$\sigma_t^2 = \frac{\alpha_2^2}{(\alpha_2-\alpha_1)^2}\frac{\sigma_N^2}{E^2}(\phi_t'(t_1)^{-2}+\phi_t'(t_2)^{-2}-\frac{2r(\tau)}{\phi_t'(t_1)\phi_t'(t_2)}), \quad (7)$$

where $\phi_t'(t_1)$, $\phi_t'(t_2)$ are the reference signal slopes determined by the signal derivations at the instants that correspond to the signal amplitude fractions α_1 and α_2, $\tau=t_1-t_2$ is time interval between samples, $r(\tau)$ is double side normalized noise correlation function. In this case the noise variance σ^2_N at the input of the discriminator is the integral of noise spectral density S(f) over the frequency band of the processor, so that $r(\tau)=R(\tau)/\sigma^2_N$, where $R(\tau)$ is double side noise correlation function that may be derived through the inverse Fourier transformation F^{-1} as $R(\tau)=F^{-1}(S(f)/2)$. The construction of the goal function for time resolution evaluation through the expression 7 is similar to that discussed for CFD in the appendix.

Conclusion

This work was motivated by intention to characterize electronic noise contribution to timing with a processor involving fraction discriminator assuming an ideal representation of the discriminator circuit. The developed approach provides a designer with a reliable estimation of time resolution dependence on the processor parameters before the back-end designing of a signal processor circuit starts. The discussed method may comprise amplitude rise time compensation technique with minor modifications. The modeling of ideal discriminator provides a possibility of rapid evaluation of front-end noise contribution to timing. The simulation method may be extended to comprise contribution of the detector signal fluctuations into timing. However certain sources of errors of other nature [8] were beyond the scope of this study. The correspondence of the simulated results to the measured values is found sufficient under the assumptions committed. The simulation results were obtained by using PSPICE version 7.1 based on Microsoft Windows platform.

Appendix. Goal function usage

The results of time resolution evaluation by goal function with the name fratr are shown in Figure 4. The goal function uses four traces to define time resolution in function of the delay for a given fraction. Parametric analysis with varying delay must precede performance analysis with the goal function. The ideal delay is introduced at the output of loaded on 50 Ohm front-end via Laplace form. The current stimulus used in parametric analysis of this study corresponds to 4.35056 Mev energy deposition in Si detector by δ-like waveform. The trace corresponding to the function under differentiation in the denominator of expression 2 is derived by corresponding macro for each fraction of interest. For each delay parameter the macro takes into account the difference of the fraction of the output waveform and the delayed output waveform. The traces corresponding to these macros are named zerconfi, where i is the number indicating the fraction. The body of the goal function with the corresponding operation comments is as follows:

```
fratr(1,2,3,4)=4.35056*(sqrt(y2)/y4)
*Marked point expression to derive
*normalized to 1 MeV time resolution. This
*is an equivalent of square root taken for both
*sides of expression 2.
{
1| search forward xval(120n) !1;
*Finds the magnitude of the trace at the
*moment of 120n; constant trace of the
*magnitude equal to the particular delay is
*used.
2| search forward xval(y1)  !2;
```

*Finds the magnitude corresponding to the *delay value; trace of pwl form representing *noise variance dependence on delay (for *fixed fraction) is used.
3| search forward (12n, 120n) level(0) !3;
*Finds the moment of zero crossing, the *limits of the search are determined by the *peaking time of the response and the range *of the delay variation; trace corresponding *to macro zerconfi is used
4| search forward xvalue(x3) !4;
*Finds the slope at the moment of zero *crossing; derivation of trace represented by *macro zerconfi is used
}

References

1.R.G.Jackson et al, IEEE Trans. on Nucl. Sci., NS-44 N3 (1997) 303-307.
2. A.R.Frolov, T.V.Oslopova, Yu.N.Pestov, Nucl Instrum. and Meth. A356 (1995) 447-451.
3. T.J.Paulus, IEEE Trans. on Nucl. Sci., v. NS-32, N3 (1985) 1242-1249.
4. J.R.Carson, Bell Syst. Tech. J., vol.10, p.374, 1931.
5. ORTEC Application Note 41. Techniques for Improved Time Spectroscopy, p.9.
6. J.Poutas et al., Nucl. Instrum. and Meth. A 369 (1996), 222-247.
7. P.W.Tuenanga, SPICE: a Guide to Circuit Simulation and Analysis Using PSPICE, Prentice-Hall, 1988, p.119.
8. D.M.Binkley and M.E.Casey, IEEE Trans. on Nucl. Sci., v. NS-35, N1 (1988) 226-230.

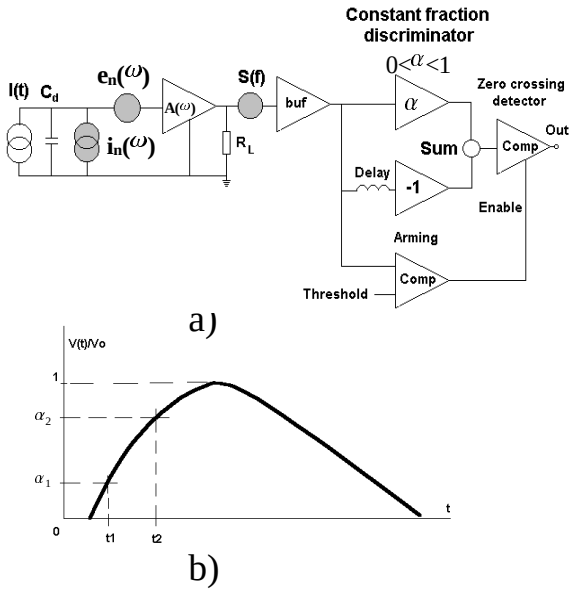

Figure 1a. A representation of a processor involving constant fraction discriminator (CFD). The front-end is loaded on 50 Ohm input impedance of CFD circuit, ideal buffer separates the input impedance from the rest of CFD circuit. Figure 1b. A principe of time mark derivation with double fraction

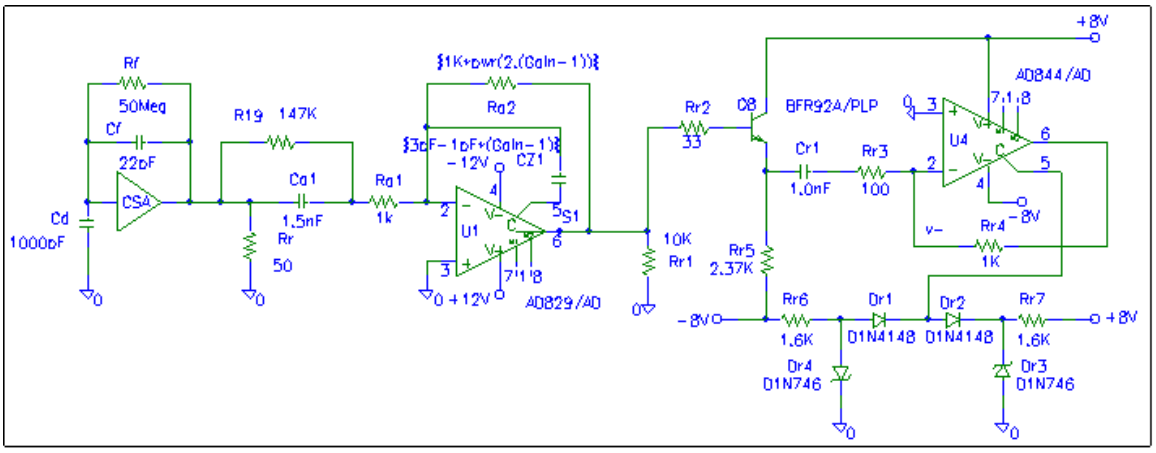

Figure 2. Schematic view of the amplifier circuit used in this study.

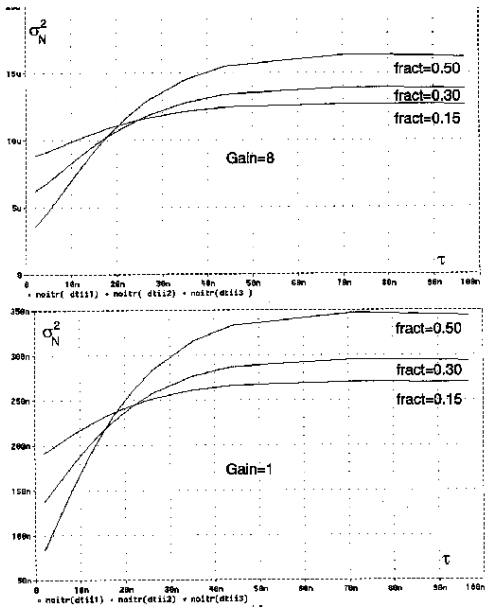

Figure 3. Front-end noise variance dependencies on delay of CFD simulated for different parameters of fraction. The data for two gain factors of the filter-amplifier are presented.

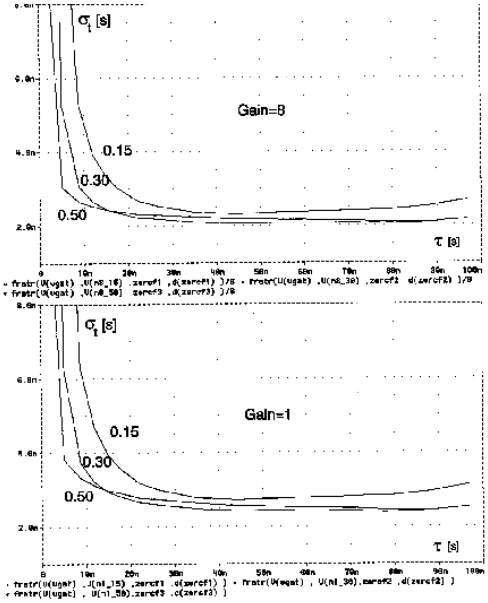

Figure 4. Time resolution (r.m.s. values) dependencies on delay of CFD presented for three parameters of fraction. Time resolution shown for two gain factors of the filter-amplifier is normalized to 1 MeV energy deposition, the stimulus is current δ-function.

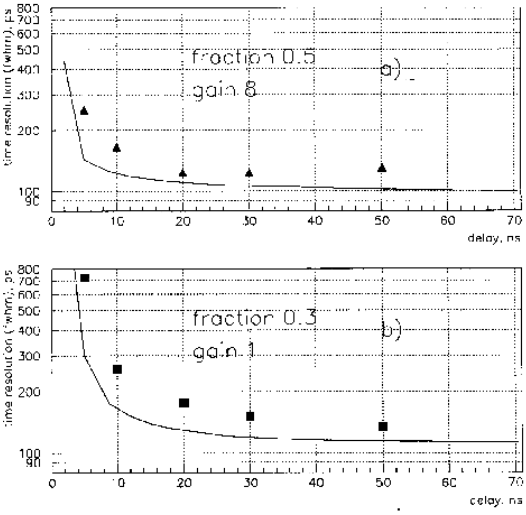

Figure 5. Simulated time resolution dependencies on delay of CFD are compared to the measured values obtained with 50 MeV stimulus. The values are presented in f.w.h.m. units. The simulated results are shown in solid lines. The measured values are shown by triangles (Figure 5a) for the filter gain factor of 8 used with 50% fraction, and by rectangles (Figure 5b) for the filter gain factor of 1 used with 30% fraction.